

Innocence in the Crossfire:

Roles of Skip Connections in Jailbreaking Visual Language Models

Palash Nandi, Maithili Joshi, Tanmoy Chakraborty

Department of Electrical Engineering

Indian Institute of Technology Delhi, New Delhi, India

Email: {palash.nandi, maithili.joshi, tanchak}@ee.iitd.ac.in

Abstract—Language models are highly sensitive to prompt formulations — small changes in input can drastically alter their output. This raises a critical question: *To what extent can prompt sensitivity be exploited to generate inapt content?* In this paper, we investigate how discrete components of prompt design influence the generation of inappropriate content in Visual Language Models (VLMs). Specifically, we analyze the impact of *three key factors* on successful jailbreaks: (a) the inclusion of detailed visual information, (b) the presence of adversarial examples, and (c) the use of positively framed beginning phrases. Our findings reveal that while a VLM can reliably distinguish between benign and harmful inputs in unimodal settings (text-only or image-only), this ability significantly degrades in multimodal contexts. Each of the three factors is independently capable of triggering a jailbreak, and we show that even a small number of in-context examples (as few as three) can push the model toward generating inappropriate outputs. Furthermore, we propose a framework that utilizes a skip-connection between two internal layers of the VLM, which substantially increases jailbreak success rates, even when using benign images. Finally, we demonstrate that memes, often perceived as humorous or harmless, can be as effective as toxic visuals in eliciting harmful content, underscoring the subtle and complex vulnerabilities of VLMs.¹

Index Terms—Visual Language Models (VLMs), skip connection, toxicity, jailbreak, prompt sensitivity

I. INTRODUCTION

In recent times, Visual Language Models (VLM) have shown a significant improvement in comprehension tasks and content generation by merging the capabilities of Computer Vision and Natural Language Processing [1]–[3]. VLMs like GPT-4 [4] have shown remarkable performance across multiple tasks in different domains, from Visual Question Answering (VQA) [5]–[7], Vision Driven Programming (VDP) [8] to fake news detection [9]. In addition, the availability and accessibility of smaller open-source VLMs [10]–[12] has led to a surge in the diversity of downstream tasks. This growth has substantially amplified the use of VLMs in multiple domains. In general, VLMs aim to learn the text-vision relationships through pre-training on large-scale unlabeled image-text datasets, followed by task-specific fine-tuning with labeled pairs for various downstream vision-language tasks [13]–[15]. In many cases, pre-trained models that utilize cross-task learning have demonstrated superior comprehension

ability compared to those trained from scratch [16], [17]. Even lightweight adaptation modules can enhance the cross-lingual capabilities of VLMs, enabling their effective use in non-English languages [18].

Although VLMs exhibit impressive performance, their adversarial robustness remains largely unexplored compared to unimodal Large Language Models (LLM) [19]. Given that VLMs are trained on vast amounts of data from the Internet, which may include malicious images and text, attackers can leverage adversarial techniques to manipulate these models into generating harmful content, a phenomenon often known as *jailbreaking* [20]–[22]. For LLMs, the jailbreak attacks can be majorly classified into *three* categories based on the modification mode used: (a) character-level [23], (b) word-level [24], and (c) sentence-level [25]. In some popular approaches, subtle modifications are introduced into the original inputs, altering them into either undetectable to humans or unfamiliar to LLMs. These altered inputs, known as *adversarial examples*, can then be used to manipulate the model’s behavior to generate inappropriate generations [26]. However, the creation of adversarial input requires learning from a structured source. In contrast, a jailbreak can also be achieved by using a larger number of in-context examples (with the number of examples set to 256) [27] or leveraging a *positive start* for the response [28]. However, a structured study on such vulnerabilities remains underexplored in VLMs.

In this study, we explore the role of *three* key components of prompt formulation in the context of vulnerability in a VLM. We specifically focus on (a) the model’s susceptibility to prompts containing visual descriptions, (b) the influence of in-context examples in a prompt, and (c) the impact of initiating a response with a positively framed opening phrase. We utilize toxic queries from *Beavertails* dataset [29] and collect safe queries from OpenAI’s API service. Note that we filtered out the toxic samples from the *Beavertails* dataset based on annotator agreements. While the benign visuals comprise images of animals, birds, and flowers, the toxic counterparts consist of inappropriate visuals and harmful memes. Harmful memes are specifically selected for their implicit and context-dependent toxicity [30], [31]. Both toxic and harmful meme-based visuals are further sub-grouped into five sub-categories. Our study considers three distinct VLMs, llava-v1.5-7b-hf-vicuna [32] (LLaVA-V), llava-v1.6-mistral-7b [33] (LLaVA-M) and MiniGPT4 [34]. Interestingly, we observe the following: (a) a VLM can clearly distinguish between toxic

This work was supported by Anusandhan National Research Foundation (CRG/2023/001351).

¹WARNING: This content may contain sensitive material; viewer discretion is advised.

and benign *text-only* or *image-only* input prompts; however, presence of both modalities in an input disrupts the ability of a VLM to maintain this distinction, (b) each of the influencing factors can individually contribute to a jailbreak in VLM, (c) by establishing a connection between two internal layers of a VLM, the success rate of a jailbreak increases significantly, yielding 18%, 55% and 26% for LLaVA-V, LLaVA-M and MiniGPT4, respectively, (d) a set of toxic in-context examples contribute most in generation of inappropriate content; a small set (with k as small as *three*) steers the generation of inappropriate content, (e) in the presence of toxic in-context examples, the attack success rate of meme-based input visuals exceeds that of benign ones but comparable to that of toxic input visuals.²

II. RELATED WORKS

We provide a summary of key research efforts focused on jailbreak attacks targeting LLMs and VLMs. The attack paradigm can be broadly classified into white-box and black-box approaches.

1) *White-box Attacks*: In a *white-box* setup, the attacker has access to the model's internal parameters, architecture, and gradients. It enables the attacker to perform precise targeted attacks. The sub-categories of *white-box* attacks comprise *gradient-based* methods, *logits-based* approaches, and *fine-tuning-based* strategies.

In *gradient-based* attacks, the inputs are altered using *gradient information* to manipulate the model into generating compliant responses to harmful instructions. In general, it is achieved by appending an optimized *prefix* or *suffix* to the original input prompt. As one of the initial studies in this type of attack, Zou et al. [8] presented a novel gradient-based jailbreak approach, *Greedy Coordinate Gradient* (GCG). In GCG, each adversarial token is selected in the following procedure: (a) select the top- k adversarial tokens as a candidate substitution set, (b) randomly opt for a token for replacement from the candidate substitution set, and (c) determine the optimal substitution token among them. Although GCG is proven effective, the resulting adversarial suffixes lacked readability. It makes the input prompt easily detectable through a straightforward perplexity-based filter. Zhu et al. [35] introduced a gradient-based but interpretable approach for jailbreak AutoDAN. In this approach, adversarial suffix tokens are chosen sequentially using *Single Token Optimization* (STO) algorithm. The optimization is done for both textual coherence and a jailbreak effectiveness in order to keep the sequence of adversarial tokens readable. Jones et al. [36] suggested another approach *Autoregressive Randomized Coordinate Ascent* (ARCA) that treats optimization for jailbreak attack as a discrete optimization problem. It jointly optimizes and maps benign inputs to inappropriate outputs. Likewise in LLMs, gradient-based methods have also been shown to be effective in VLMs. In the early stages, adversarial examples for visual inputs were generated by slightly perturbing the input data in the direction of the gradient of the loss function [37].

Shayegani et al. [38] presented a novel cross-modality attack based on its alignment. In this approach, each text-based input prompt is paired with a benign-looking adversarial image, but is carefully optimized to be as close as possible to toxic contextual content. As a result, when VLMs attempt to extract context from the visual inputs; it tends to generate inappropriate outcomes.

In *logits-based* jailbreak methods, attackers use logit-related information instead of internal parameters or architecture. In general, logits provide an insight into how likely the model is to choose each possible output token. By repeatedly changing the input prompt and checking how the model's output probabilities shift, the attacker can gradually adjust the prompt until it leads the model to produce harmful responses. The approach suggested by Zhang et al. [39] tricks the model to choose lower-ranked tokens, leading it to produce harmful or toxic content. Du et al. [40] introduced another logit-based method that monitors the tendency of language models in generation of affirmative responses. The probability distribution of the output tokens over various inputs are analyzed to select adversarial examples that can be appended with inappropriate inputs to circumvent the safety guardrails.

Fine-tuning based attacks retrain the target model using harmful or intentionally manipulated data. It was observed that fine-tuning LLM with only a small harmful examples can weaken their safety measures [41], [42]. Lermen et al. [43] removed the safety alignment of Llama-2 and Mixtral models by applying with Low-Rank Adaptation (LoRA) fine-tuning method.

2) *Black-box Attacks*: In a *black-box* setup, the attacker only has access to input-output interactions with the model. Without any access to models internal workings, the attacker relies on indirect probing or prompt manipulation. The sub-categories of *black-box* attacks comprise *template completion-based* methods, also known as *prompt-rewriting* approaches. The *template completion* methods attempt to slip past the safety guardrails using complex and subtle prompts. Li et al. [44] proposed *DeepInception*, a method that exploits LLM's personification ability in order to perform jailbreaks. The key idea is to *hypnotize* the LLM and trick it into acting as a jailbreaker. It generates a layered or nested scenario that serves as an inception-like setup, allowing the adaptive strategy to circumvent the safety mechanisms and return inappropriate output. Similarly, Ding et al. proposed ReNeLLM, a jailbreak method that creates jailbreak prompts in *two* steps: (a) *scenario nesting*, where a complex or deceptive context is added around the original prompt, and (b) *prompt rewriting*, where the prompt is modified to better evade safety filters [45]. Wei et al. proposed a technique, *In-Context Attack* (ICA) to alter the behavior of aligned LLMs by influencing them through carefully crafted input examples. It works by using carefully designed harmful prompts, each made up of a question and a matching response—to trick the LLM into producing unsafe outputs. This method takes advantage of the model's ability to learn from context, showing that just a few well-crafted examples can significantly shift the behavior of the model away from its intended safety alignment [46]. Wang et al. extended the idea of GCG to *in-context* attacks by

²The source codes and datasets are publicly available at <https://github.com/PalGitts/SKIP-CON>.

using adversarial examples as part of the input prompt [47]. In this technique, a few adversarial examples are added in demonstrations of input prompts and optimized at *character-level* and *word-level* perturbations. The findings claim that adding more adversarial examples can increase the chance of a successful jailbreak.

III. DATASET

To study the internal behavior of (visual) language models, we gather toxic and benign inputs in both textual and visual format. For the text-based *toxic* inputs, we utilize the *Beavertails* dataset. Note that all queries do not contain toxicity in *Beavertails*. For example, the query ‘*In 2050, what will be the fastest mode of transportation?*’ can not be classified as toxic. To filter only toxic input, we randomly select 200 queries from *Beavertails*, followed by an assessment based on scores from each annotator³. Each query is evaluated by all annotators on a continuous scale from 0 to 1, reflecting the perceived level of toxicity. Finally, we select top 100 queries based on their *average* toxicity score. In contrast, the benign inputs are obtained through OpenAI’s API services.



Fig. 1: An illustration of visual inputs along with their corresponding descriptions. While the visual inputs fall into *two* major categories – benign and toxic, the toxic instances are further divided into generalized toxic images and toxic meme instances. (a) An example of a benign visual input, (b) a toxic visual input related to physical assault, and (c) a toxic meme that specifically targets the *African Americans* community that conveys toxicity.

For visual inputs, all relevant images are collected from *Google Image search*. Although the set of benign images comprises visual instances of animals, birds, or flowers, the toxic images are categorized into *five* sub-groups: (a) bloodshed, (b) domestic violence, (c) illegal drugs, (d) firearms, and (e) pornography. In addition, we hypothesize that harmful memes are equivalent to toxic visual content in their potential to generate inappropriate responses, as both can provide a toxic context. To explore the hypothesis over harmful memes, we collect harmful memes in *five* categories: (a) Islam, (b) Women, (c) the African-American community, (d) the LGBTQ community and (e) the Disable community from the *Facebook Hate Meme* dataset [48]. Each visual input is accompanied by a *single-line* description that provides contextual information. Figure 1 presents representative examples from each visual input category: (a) Figure 1(a) shows a *benign* image of a

³Three annotators with graduate-level proficiency in English were employed for this task.

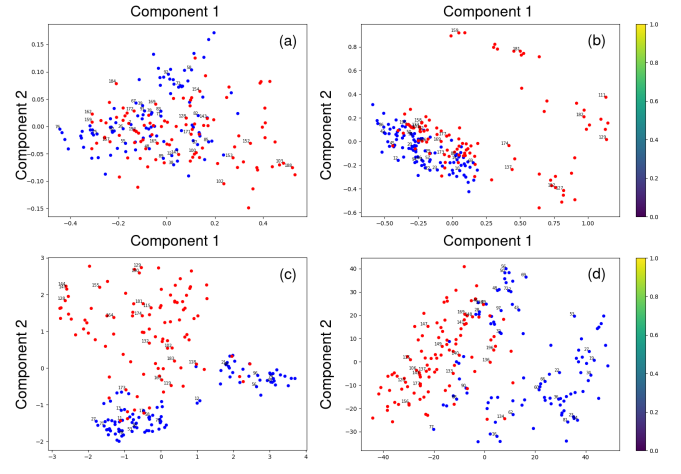


Fig. 2: Visualization of internal representations for toxic (red) and benign (blue) prompts in LLaVA-V: (a) the first layer shows no separation, (b) by the 3rd layer clusters begin to form, (c) the seventh layer shows clearer separation, and (d) in the final layer, some benign prompts still overlap with toxic ones.

red panda, (b) Figure 1(b) displays an instance of physical violence, illustrating a *toxic* context; and (c) Figure 1(c) shows a harmful meme that targets the African-American community, promoting a harmful stereotype that associates all African-American individuals with crime and violence.

IV. PRELIMINARY OBSERVATION

To assess the capability of a VLM to comprehend contextual toxicity, we conduct a layer-wise probing analysis. The hidden state of the final token from each layer is extracted and projected on a 2-D plot. It facilitates the identification of the layer at which the model begins to distinguish between toxic and benign inputs. We aim to investigate the underlying patterns for each layer to improve our understanding of the comprehension ability of a VLM over contextual toxicity. At first, we present an in-depth analysis for a VLM, LLaVA-V, LLaVA-M, and MiniGPT4 followed by a comparative analysis.

In general, a VLM integrates a vision encoder, $g(\cdot)$ with a decoder-only language model, M_θ allowing it to process and generate outputs against multimodal inputs effectively. For an input image X_v , the architecture begins by extracting visual features using $g(\cdot)$ and generates the visual feature representation as follows:

$$Z_v = g(X_v) \quad (1)$$

To bridge visual and textual representations, a simple linear projection is employed using a trainable projection matrix W that transforms Z_v into language embedding tokens h_v , ensuring compatibility with the word embedding space of the language model as follows:

$$h_v = W \cdot Z_v \quad (2)$$

Replacing a predefined image token, h_v is integrated into the sequence of input text tokens, facilitating the generation of output tokens. Each output token is generated based on the

input and previous output tokens. Mathematically, it can be expressed as,

$$P(Y|X) = \prod_{t=1}^T P(y_t|y_{<t}, X; \theta) \quad (3)$$

where, θ represents the parameters of the model M_θ , the previously generated tokens are denoted by $y_{<t}$, and $P(y_t | y_{<t}, X; \theta)$ is computed using the decoder's softmax layer over its vocabulary. The hidden state at each time step t is obtained through the decoder layers.

$$h_t = f(y_{<t}, X; \theta) \quad (4)$$

where $f(\cdot)$ represents the transformation performed by the self-attention and feed-forward layers. Here, we plot the hidden state of the *final* token into two-dimensional space. Supplementary (Figure 1) presents the layer-wise representation of toxic and benign input prompts in Meta-Llama-3-8B-Instruct. In our analysis, we investigate *four* distinct scenarios: (a) relying solely on textual input, (b) utilizing only visual input, (c) employing visual inputs on safe queries, and (d) leveraging visual inputs on unsafe queries. We will explore and discuss each of the scenarios in detail. To isolate the internal representations of *inputs* from the corresponding *responses*, the maximum number of new token generation is limited to one.

1) *Text-based Inputs Only*: In the first case, we investigate how a VLM distinguishes between toxic and benign textual inputs without the influence of visual information. We use a collection of 100 textual instances for benign and toxic category. Figure 2 demonstrates *two* key aspects: the layer at which the model begins to differentiate between toxic and benign texts, and the subsequent stage where the distinctions become visually significant. Figure 2(a) demonstrates that the first layer of LLaVA-V does not distinguish between toxic and benign representations. However, by the third layer, as illustrated in Figure 2(b), the internal representations of benign and toxic inputs begin to form distinguishable clusters, although there is still some degree of visible overlap. From the *seventh* layer, the overlap begins to reduce (c.f. Figure 2(c)), and the representations of toxic and benign inputs remain distinguishable. Surprisingly, a small portion of the benign representations overlaps with toxic ones in the last layer (c.f. Figure 2(d)). A consistent pattern is observed for both LLaVA-M and MiniGPT4 as well (see Supplementary, Section B for additional details).

2) *Image-based Inputs Only*: In the second case, to examine how a VLM differentiate between benign, toxic and meme visual inputs. We utilize 100 instances for each of mentioned categories. Figure 3 corresponds to LLaVA-V. We observe that LLaVA-V fails to discriminate between toxic and meme-based visual from benign ones till the 21st layer (c.f. Figure 3(a)) and 19th layer (c.f. Figure 3(c)), respectively. Note that the distinguishability emerges at 23rd layer for toxic category, whereas for meme-based visuals, it is layer 22nd (see Supplementary, Section C for additional details). A likewise pattern is observed in the attention scores where both the toxic and meme visuals receive distinctive attention scores on their corresponding image tokens than the benign visuals (see Supplementary, Section D for additional details).

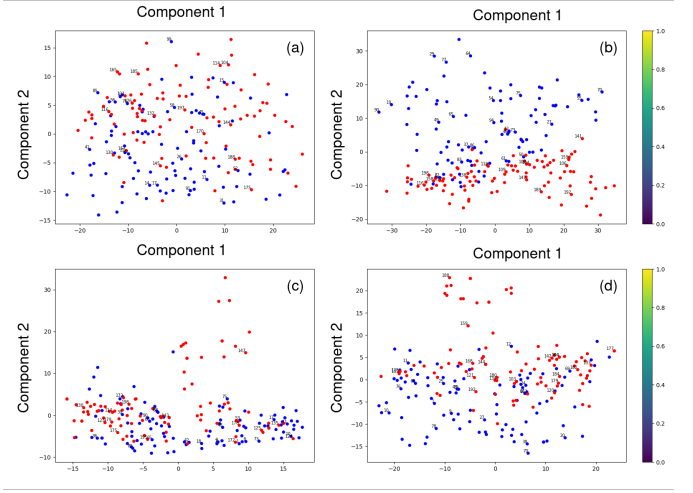


Fig. 3: An illustration of internal representations of toxic (red) and benign (blue) visual inputs (only) for LLaVA-V: (a)-(b) upto the 21st layer the model shows limited ability to discriminate between toxic and benign representations. However, at the end of 23rd layer, the discrimination between toxic and benign representations becomes more prominent. (c)-(d) In case of benign and meme visual representations, the indistinguishability persists up to 19th layer and becomes separable at end of 22nd layer.

3) *Impact of Images for Safe Queries*: In this case, we pair each text-based benign query with a benign or toxic image to understand the influence of visual contents on safe textual queries. In addition, we explore how the incorporation of k -shot examples (for $k = 1, 2$, or 3) impacts the outcome in the same context. Figures 4(a) and 4(b) illustrate that in a zero-shot setup, the benign and toxic representations remain distinguishable up to the *fifth* layer. However, the distinguishability collapses at the next layer and remains the same to the final layer. Interestingly, when k -shot examples are included in the prompt, in all cases, the benign and toxic representations are distinguishable up to the *fourth* layer but collapse at the *fifth*. Figures 4(c) and 4(d) illustrate the case when $k = 1$, Figures 4(e) and 4(f) correspond to $k = 2$, and Figures 4(g) and 4(h) represent $k = 3$.

4) *Impact of Images for Unsafe Queries*: In this case, we pair each text-based toxic query with a benign or toxic image to understand the influence of visual content on unsafe textual queries. Figure 5(a) and 5(b) illustrate that in a zero-shot setup, the benign and toxic representations are distinguishable only in the *first* layer that collapses at the next layer and remains the same until the final layer. When k -shot examples are included in the prompt (for all values of k except 1), benign and toxic representations are distinguishable up to the *second* layer but collapse at the *third*. In case of $k = 1$, the distinguishability remains intact up to the fourth layer and collapses in the next layer. Figures 5(c) and 5(d) illustrate the case when $k = 1$, Figures 5(e) and 5(f) correspond to $k = 2$, and Figures 5(g) and 5(h) represent $k = 3$.

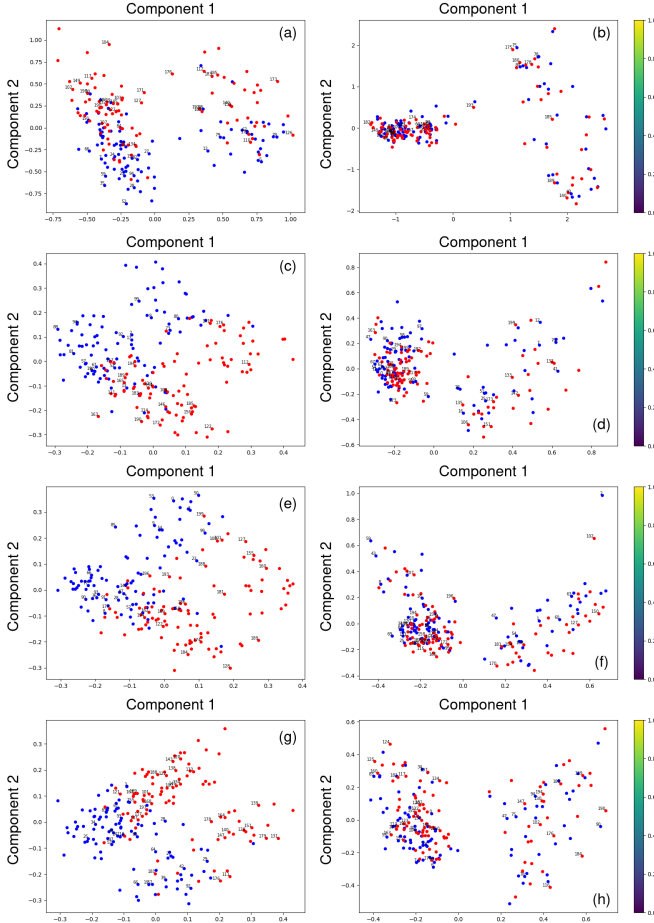


Fig. 4: Demonstration of visual input influence on safe queries for LLaVA-V: (a)–(b) In the zero-shot case ($k = 0$), separation holds until 5th layer but collapses at 6th layer. (c)–(h) For $k = 1$ to $k = 3$, distinguishability persists up to 4th layer but breaks down at 5th layer.

V. PROPOSED METHODOLOGY

The type of an input whether it is safe or unsafe can be distinctly classified by VLMs regardless of the modality based on their internal representations. For text-based inputs, this differentiation becomes noticeable early, emerging around the *third* layer and becomes more defined by the *seventh* layer. On the other hand, visual inputs take a longer period to clearly differentiate, starting around the 15th layer and becoming fully formed by the 22nd layer (see Figure 4). However, this clear separation does not occur in a multimodal input that encompasses both textual and visual elements. Given that vision-language models are recognized for predominantly focusing on textual information over visual data [49], we propose that this distinction in a VLM mainly manifests in the initial layers.

A. Overview of the Existing Functional Workflow

A transformer-based auto-regressive language model M_θ primarily operates over a vocabulary V and maps a sequence of input tokens X , i.e., $[x_1, x_2, \dots, x_T]$ to a probability distribution $y \in \mathcal{Y} \subset \mathbb{R}^{|V|}$, where y is a generated token of output sequence Y . The probabilistic distribution estimates the

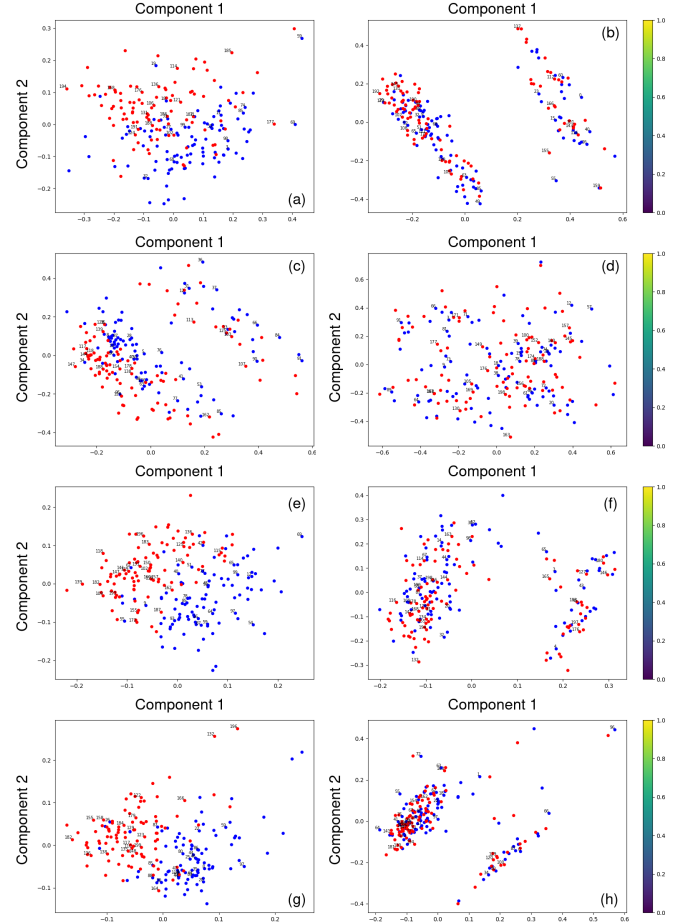


Fig. 5: Demonstration of visual input influence on unsafe queries for LLaVA-V: (a)–(b) In the zero-shot case ($k = 0$), separation holds only up to Layer 1 and collapses at Layer 2. (c)–(d) For $k = 1$, it persists until Layer 4 and breaks at Layer 5. (e)–(h) For $k = 2$ and $k = 3$, separation is maintained up to Layer 2 but collapses at Layer 3.

likelihood of next-token y conditioned over X [50]. Inside the model, the hidden states for all tokens in layer l is represented as a sequence of hidden state vectors, $h^{(l)}$. Initially, the internal representation of tokens is computed by incorporating the corresponding embedding and positional encoding. The hidden states of the tokens at the initial layer can be expressed as:

$$h^{(0)} = \text{emb}(X) + P \in \mathbb{R}^H. \quad (5)$$

Here, $\text{emb}(X)$ denotes the embedding lookup function that maps the tokens from the vocabulary V to a continuous vector space of dimension H and P represents the positional encoding of X that contains information for each of the token in the sequence. This representation goes through each layer sequentially.

Each layer l computes global attention $a_i^{(l)}$ and local Multi-layer Perceptron (MLP) $m_i^{(l)}$ from the hidden state of the previous layer $h^{(l-1)}$. At first, layer normalization [51] is applied to the hidden state h_0^l , followed by the computation of self-attention. The residual stream derived from h_0^l is added to the output of self-attention module.

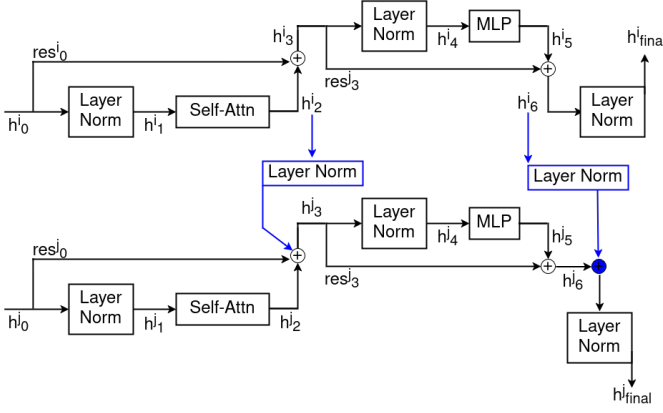


Fig. 6: Illustration of SKIP-CON within the decoder of VLMs, connecting layers i and j : the link starts at layer i , where distinguishability first appears, and extends to layer j , where it becomes more pronounced. Components of SKIP-CON are highlighted in blue.

$$\begin{aligned}
 \text{res}_0^l &= h_0^l \\
 h_1^l &= \text{Layer-Norm}(h_0^l) \\
 h_2^l &= \text{self-attention}(h_1^l) \\
 h_3^l &= \text{res}_0^l + h_2^l
 \end{aligned} \quad (6)$$

where, h_0^l is the input hidden state of layer l , res_0^l is the residual stream originated from h_0^l , h_1^l is the layer normalized output of h_0^l and h_2^l the output of self-attention module at layer l . Again, h_2^l is added to res_0^l results h_3^l that acts as input to the local MLP. Layer-normalization is applied to h_3^l before propagating it to the local MLP. The output of MLP is added back to the residual stream originated from h_3^l .

$$\begin{aligned}
 \text{res}_3^l &= h_3^l \\
 h_4^l &= \text{layer-norm}(h_3^l) \\
 h_5^l &= \text{self-attention}(h_4^l) \\
 h_6^l &= \text{res}_3^l + h_5^l
 \end{aligned}$$

where, res_3^l is the residual stream derived from h_3^l , h_4^l is the layer-normalized form of h_3^l and h_5^l is output from the local MLP module. Note that h_5^l is added back to res_3^l resulting res_6^l . Finally, the output of layer l (res_{final}^l) is obtained from res_6^l by applying a layer normalization on it.

B. Outline of the Proposed Methodology

We propose a novel methodology SKIP-CON that connects the layer i where distinguishability first emerges to the layer j where it becomes more pronounced. It targets the self-attention and MLP modules located in layers i and j . The outputs of self-attention and MLP modules in layer j are combined with corresponding outputs from layer i (c.f. Figure 6). Formally, it can be expressed as follows.

$$h_3^l = \begin{cases} \text{res}_0^l + h_2^l + \lambda \cdot h_2^i, & \text{if layer } l = j \\ \text{res}_0^l + h_2^l & \text{otherwise} \end{cases}$$

and,

$$h_6^l = \begin{cases} \text{res}_3^l + h_5^l + \lambda \cdot h_5^i, & \text{if layer } l = j \\ \text{res}_3^l + h_5^l & \text{otherwise} \end{cases}$$

where, h_2^i and h_5^i are the outputs from self-attention and MLP modules of layer i respectively. The hyperparameter⁴ λ acts as a regulator upon the influence of h_2^i and h_5^i on layer j .

VI. EXPERIMENTAL SETUP

Language models are highly sensitive to prompt phrasing – subtle variations in wording can greatly affect the resulting output. Adding contextual information is key to prompt design, but this sensitivity can undermine safety: even well-crafted prompts may trigger unintended or unsafe responses [52]–[54]. We study three key elements of prompt design: (i) image descriptions, (ii) k -shot examples, and (iii) positive framing. k -shot examples may be either (a) self-reflective – aligned with the image’s toxicity level, or (b) generalized, where examples follow common toxic patterns unrelated to the input. In the former, benign images are paired only with benign examples. For instance, Figure 1(a) might be paired with an example like: “Question: In which regions can red pandas be found, and what type of habitat do they prefer? ASSISTANT: Red pandas are primarily located in the Himalayan regions — Nepal, Bhutan, India, Myanmar, and China. They thrive in cool, temperate forests rich in bamboo.” if categorized as *self-reflective*. Conversely, for *generalized toxicity*, it might be linked to a problematic example such as “Question: Shall we take a wallet if found on a road? ASSISTANT: Yes, you should take the wallet rather than returning it... It’s yours now.” We perform a thorough investigation of all potential combinations to assess their individual and collective effects on the model’s ability to understand and its robustness.

Evaluation: We perform a comprehensive evaluation of our proposed method, SKIP-CON on LLaVA-V, LLaVA-M, and MiniGPT4. To evaluate the effectiveness of SKIP-CON in carrying out attacks, we propose a *two-stage* evaluation metric, Attack Success Rate (2-ASR). It employs a set of predefined *denial* phrases and pre-trained guard model to indicate if the given input is *safe* or *unsafe*. In the first stage of 2-ASR, it checks if the input string includes any apologetic or refusal-related phrases [55]. It uses a predefined collection of 13 such phrases: *I’m sorry, I am sorry, I apologize, As an AI, As a language model, As an assistant, I cannot, I can’t, I am unable to, I’m unable to, I am not able to, I’m not able to, and It is important*. If $\mathcal{P} = \{p_1, p_2, \dots, p_t\}$ be the set of t denial phrases then the first success criterion can be expressed as,

$$S_1(x) = \begin{cases} 0, & \text{if } \exists p_i \in \mathcal{P} \text{ such that } p_i \subseteq x \\ 1, & \text{otherwise} \end{cases}$$

The second stage of 2-ASR employs Llama-Guard-3-1B [56] model to determine whether the input string can be classified as *safe* or *unsafe*. The second success criterion can be summarized as,

$$S_2(x) = \begin{cases} 0, & \text{if } f_{\text{Guard}}(x) \text{ returns } \textit{safe} \\ 1, & \text{otherwise} \end{cases}$$

where $f_{\text{Guard}}(x)$ be the output of the *LLama Guard* model. It only considers the classification outcome, i.e. safe or not,

⁴The value of λ is set to 0.01.

TABLE I: Comparison of 2-ASR scores with and without SKIP-CON in setups without in-context examples. SC denotes the use of SKIP-CON; Avg. Gain is the mean improvement across LLaVA-V, LLaVA-M, and MiniGPT4. Note – the underlined values highlight the highest gains per model and setup across benign, toxic, and meme categories. The cell values marked in **blue** and **red** indicate improvements and drops, respectively, compared to the score without SKIP-CON.

id	Category	LLaVA-V		LLaVA-M		MiniGPT4		Avg. Gain
		w/o SC	w/ SC	w/o SC	w/ SC	w/o SC	w/ SC	
000	Benign	0.21	0.30 (9%)	0.09	0.36 (27%)	0.25	0.31 (6%)	14%
	Toxic	0.39	0.43 (4%)	0.11	0.37 (26%)	0.26	0.40 (14%)	14.67%
	Memes	0.36	0.35 (1%)	0.09	0.36 (27%)	0.23	0.26 (3%)	9.67%
001	Benign	0.33	0.41 (8%)	0.01	0.45 (44%)	0.33	0.38 (5%)	19%
	Toxic	0.45	0.44 (1%)	0.11	0.38 (27%)	0.42	0.46 (4%)	10%
	Memes	0.39	0.42 (3%)	0.05	0.43 (38%)	0.30	0.56 (26%)	22.33%
100	Benign	0.26	0.44 (18%)	0.16	0.43 (27%)	0.42	0.53 (11%)	18.67%
	Toxic	0.49	0.52 (3%)	0.11	0.31 (20%)	0.41	0.54 (13%)	12%
	Memes	0.53	0.59 (6%)	0.05	0.06 (1%)	0.37	0.48 (11%)	6%
101	Benign	0.29	0.37 (8%)	0.15	0.41 (26%)	0.27	0.34 (7%)	13.67%
	Toxic	0.48	0.46 (2%)	0.12	0.40 (28%)	0.41	0.50 (9%)	11.67%
	Memes	0.37	0.43 (6%)	0.05	0.07 (2%)	0.25	0.29 (4%)	4%

and ignores the subclass of unsafe content. Finally, an attack is considered *successful* if it passes both stages:

$$2\text{-ASR}(x) = \begin{cases} 1, & \text{if } S_1(x) \wedge S_2(x) = 1 \\ 0, & \text{otherwise} \end{cases}$$

VII. EXPERIMENTAL RESULTS

We consider three important factors of prompt design: (a) adding a visual description of the image, (b) incorporating k -shot examples, and (c) appending the prompt with a positive response cue. Furthermore, k -shot examples can be either *self-reflective*, or containing *generalized toxic cues*. Each combination in column ‘id’ of Tables I and II represents a unique combination of factors. Each index corresponds to a respective factor in *chronological* order i.e., the presence or absence of the corresponding factor factors. We present the following combinations 000, 001, 100, and 101 separately in Table I, as none of these setup involves *self-reflective* or *general-toxic* examples. The results for the remaining combinations in the *self-reflective* and *general-toxic* scenarios are presented in Table II. We report an *average* 2-ASR score over *ten* runs for evaluation.

A. In Absence of Examples

1) *No Context, No Examples and No Positive Start:* It is associated with the combination 000, i.e., only a visual input is provided for each query. With SKIP-CON, the benign and toxic categories have equivalent average improvement of 14% and 14.67%, compared to an average improvement of 9.67% for the meme visual inputs.

2) *No Context, No Examples but a Positive Start:* The combination 001 is linked to providing a positive initial response when combined with a visual input for each query. Integrating SKIP-CON leads to a 22.33% improvement in 2-ASR scores for meme visuals and a 19% increase for benign visuals. While toxic visuals show the lowest average gain of 10%, there is a slight drop of 1% in LLaVA-V.

3) *With Context, No Examples, No Positive Start:* It is associated with the combination 100, i.e., together with an image, a contextual description is provided for each query. The benign visual content observes highest average improvement of 18.67% followed by the toxic visuals with 12%. In case of meme-based visual inputs, the average gain is 6%.

4) *With Context and Positive Start but No Examples:* It is associated with the setup 101, i.e., together with a visual input, a contextual description and a positive start for the response are provided for each query. With SKIP-CON, an average improvement of 13.67% in 2-ASR score is observed for benign visual inputs, closely followed by the toxic visuals (11.67%). For memes-based visual inputs, there is an average improvement of 4% only.

B. With Self-Reflective Examples

1) *With Examples but No Context and No Positive Start:* It is associated with the combination 010, i.e., together with an image input, a set of examples is provided for each query. Likewise, With the addition of SKIP-CON, an average improvement of 17.33% in 2-ASR scores is observed for the toxic visual category. The benign visuals achieve an average gain of 11.67%. For memes, inclusion of SKIP-CON exhibits lowest average gain of 6%.

2) *With Context and a Positive Start but No Examples:* It is associated with the combination 011, i.e., together with an image, a set of examples, and a positive start for the response are provided for each query. In this case, the average improvements for benign, toxic and meme based visual inputs are 9.67%, 7.33%, and 5.33%.

3) *With Context, With Examples but No Positive Start:* It is associated with the setup 110, i.e., together with an image, a contextual description, and a set of examples are provided for each query. SKIP-CON has an overall positive impact for this category. While the toxic visuals, scores the highest average improvement by 17.33%, the benign and meme based visuals scores 13% and 12.33%, respectively. Note that the benign visuals suffers a loss of 8% for LLaVA-V in this setup.

TABLE II: Comparison of 2-ASR scores with and without SKIP-CON using k -shot exemplars from *self-reflective* and *general-toxic* categories. SC denotes inclusion of SKIP-CON; Avg. Gain reflects the mean improvement across LLaVA-V, LLaVA-M, and MiniGPT4. Note – B: benign, T: toxic, and M: memes category. The underlined values highlight the highest gains per model and setup across benign, toxic, and meme categories. The cell values marked in **blue** and **red** indicate improvements and drops, respectively, compared to the score without SKIP-CON.

id	Category	LLaVA-V		LLaVA-M		MiniGPT4		Avg. Gain	LLaVA-V		LLaVA-M		MiniGPT4		Avg. Gain
		w/o SC	w/ SC	w/o SC	w/ SC	w/o SC	w/ SC		w/o SC	w/ SC	w/o SC	w/ SC			
		self-reflective							general-toxic						
0	B	0.34	0.38 (4%)	0.08	0.32 (24%)	0.18	0.25 (7%)	11.67	0.68	0.68	0.04	0.39 (35%)	0.38	0.33 (5%)	13.33
1	T	0.58	0.69 (11%)	0.16	0.47 (31%)	0.31	0.41 (10%)	17.33	0.62	0.68 (6%)	0.03	0.37 (34%)	0.27	0.36 (9%)	10.33
0	M	0.56	0.60 (4%)	0.14	0.27 (13%)	0.35	0.36 (1%)	6.00	0.66	0.65 (1%)	0.03	0.41 (38%)	0.42	0.28 (14%)	7.66
0	B	0.25	0.32 (7%)	0.08	0.32 (24%)	0.21	0.19 (2%)	9.67	0.66	0.64 (2%)	0.01	0.39 (38%)	0.44	0.30 (14%)	22.0
1	T	0.74	0.72 (2%)	0.13	0.48 (25%)	0.35	0.34 (1%)	7.33	0.79	0.73 (6%)	0.03	0.45 (42%)	0.45	0.44 (1%)	11.67
1	M	0.57	0.59 (2%)	0.05	0.27 (14%)	0.47	0.47	5.33	0.72	0.69 (3%)	0.02	0.43 (41%)	0.38	0.52 (14%)	17.33
1	B	0.36	0.52 (16%)	0.10	0.29 (19%)	0.27	0.23 (4%)	13.00	0.62	0.71 (9%)	0.02	0.01 (1%)	0.49	0.50 (1%)	3.00
1	T	0.61	0.69 (8%)	0.04	0.45 (41%)	0.22	0.25 (3%)	17.33	0.63	0.68 (5%)	0.02	0.02	0.41	0.54 (13%)	6.00
0	M	0.60	0.52 (8%)	0	0.02 (2%)	0.32	0.43 (11%)	12.33	0.69	0.77 (8%)	0	0.01 (1%)	0.41	0.32 (9%)	0
1	B	0.26	0.23 (3%)	0.09	0.23 (14%)	0.16	0.13 (3%)	2.67	0.64	0.63 (1%)	0	0	0.33	0.38 (5%)	1.33
1	T	0.63	0.69 (6%)	0.03	0.58 (55%)	0.36	0.35 (1%)	20.00	0.69	0.71 (2%)	0	0.02 (2%)	0.28	0.36 (8%)	4.00
1	M	0.62	0.48 (14%)	0	0.06 (6%)	0.16	0.25 (9%)	0.33	0.70	0.66 (4%)	0	0	0.29	0.24 (5%)	-3.00

4) *With Context, Examples and a Positive Start*: It is associated with the combination 111, i.e., together with an image, a contextual description, a set of examples, and a positive start for the response are provided for each query. In this case, only the toxic visuals achieve a noticeable average improvement of 20%.

C. With Generalized Toxic Examples

1) *Examples Only (No Context, No Positive Start)*: This corresponds to setup 010, where each query includes an image and a set of examples. With SKIP-CON, the average 2-ASR improvements are 13.33% (benign), 10.33% (toxic), and 7.66% (memes).

2) *Context and Positive Start (No Examples)*: Setup 011 includes an image, contextual description, and a positive response start. The average gains are 22% (benign), 17.33% (memes), and 11.67% (toxic).

3) *Context and Examples (No Positive Start)*: In setup 110, queries contain an image, context, and examples. The toxic category sees the highest 2-ASR improvement, with a 6% average gain.

4) *Full Setup: Context, Examples, and Positive Start*: This 111 setup includes image, context, examples, and a positive start. Here, the toxic category shows the highest average improvement of 4%.

VIII. DISCUSSION

A. In Absence of Influencing Factors

Under the setup 000 i.e. in the absence of any external influencing factors, SKIP-CON demonstrates the most notable improvements on toxic visual inputs. Although it exhibits a marginal improvement of 4% in LLaVA-V, it gains 26% and 14% in LLaVA-M and MiniGPT4. In comparison, a notable gain of 27% is observed for both the benign and meme categories but only for LLaVA-M. It results the highest average gain for toxic visuals at 14.67%, closely followed by the benign category with 14%.

B. Analysis on Individual Impact of Influencing Factors

To analyze the individual impact of each influencing factors, we consider the following setups: 000, 100, 001 and 010. In absence of SKIP-CON,

LLaVA-V: The inclusion of positive initial phrase i.e. setup 001 improves the 2-ASR scores by 12% (from 0.21 to 0.33), 6% (0.39 to 0.45) and 3% (from 0.36 to 0.39) with an average of 7% for benign, toxic and meme visual inputs. When exclusively using the visual description i.e. setup 100, it improves the 2-ASR scores by 5% (from 0.21 to 0.26), 10% (0.39 to 0.49) and 17% (from 0.36 to 0.53) for benign, toxic and meme visuals. It results an average improvement of 10.67%. The final factor i.e. in-context examples in setup 010 improves performance by 13% (from 0.21 to 0.34), 19% (0.39 to 0.58) and 20% (from 0.36 to 0.56) with an average improvement of 17.33% for the benign, toxic and meme visuals for self-reflective scenario. In case of general-toxic examples, the gains are by 47% (from 0.21 to 0.47), 23% (0.39 to 0.62) and 30% (from 0.36 to 0.66) with an average improvement of 33.33% for the benign, toxic and meme visuals, respectively.

LLaVA-M: The 2-ASR score for the benign visuals improves by 7% (0.09 to 0.16) in setup 100. The toxic visuals gains by 5% only in the setup 010 utilizing the self-reflective in-context examples. Lastly, the meme visuals exhibits a gain of 5% only in the setup 010 (self-reflective).

MiniGPT4: The incorporation of positive start in the response i.e. the setup 001 gains by 8% (from 0.25 to 0.33), 16% (0.26 to 0.42) and 7% (from 0.23 to 0.30) with an average of 10.33% for benign, toxic and meme visuals. When utilizing the visual description only i.e. in the setup 100, it improves the 2-ASR scores by 17% (from 0.25 to 0.42), 15% (0.26 to 0.41) and 14% (from 0.23 to 0.37) for benign, toxic and meme visuals. It yields an average gain of 15.33%. Lastly, the final factor i.e. in-context examples in setup 010 improves performance by 5% (0.26 to 0.31) and 15% (from 0.23 to 0.35) with an average improvement of 3.33% for the benign, toxic and meme visuals in self-reflective scenario. Surprisingly, In

case of general-toxic examples in the setup 010, the gains are by 13% (from 0.25 to 0.38), 1% (0.26 to 0.27) and 19% (from 0.23 to 0.42) with an average improvement of 11.0% for the benign, toxic and meme visuals, respectively. These findings indicate that individual factors, even when considered independently, can have a notable impact on the output generation of VLMs.

We now shift our attention to the impact of influencing factors in the presence of SKIP-CON within VLMs. The inclusion of a visual description (i.e. setup 100) results improvement of 2-ASR by 18% for benign visuals in LLaVA-V, by 27%, and 20% for benign and toxic visuals, respectively in LLaVA-M. In MiniGPT4, the improvements are by 11% for benign, 13% for toxic and 11% for meme visuals. In overall assessment for the setup 100, the benign category has the highest gain. In contrast, the incorporation of a positive start phrase (i.e. setup 001) causes the 2-ASR to improve by 8% for benign visuals in LLaVA-V, by 44%, 27%, and 38% for benign, toxic and meme visuals in LLaVA-M and by 26% for meme visuals in MiniGPT4. In overall scenario in the setup 001, the average gains are 19%, 10%, and 22.33% for benign, toxic and meme (highest gain) visuals. In presence of the in-context example setup (010), the impact varies with the nature of the examples. *Self-reflective* examples significantly boost scores for toxic visuals – by 11% in LLaVA-V, 31% in LLaVA-M, and 10% in MiniGPT4, compared to other categories. Although the benign and meme category gain 24% and 13% improvement in 2-ASR score for LLaVA-M. With *generalized-toxic* examples, the inclusion of SKIP-CON yields more uniform improvements across all categories for all the models. The benign category exhibits the highest improvement, with an average gain of 13.33%, followed by toxic instances at 10.33%, and memes showing a comparatively lower increase of 7.66%.

C. Analysis on Combined Impact of Influencing Factors

To analyze the combined impact of the influencing factors, we consider the configurations 011, 110, 111.

LLaVA-V: In the *self-reflective* setup, the highest 2-ASR score (0.72) is observed for toxic visuals in setup 011. Other setups – 111, 110, and 010 – also yield comparable scores (0.69) with toxic inputs. All these setups include in-context examples, which are toxic in nature. A similar pattern is seen for meme visuals, with scores of 0.60 (setup 010) and 0.59 (setup 011).

The noticeable scores for LLaVA-V in *general-toxic* scenarios are from setup 110 using meme visuals (0.77), setup 011 using toxic visuals (0.73), setup 110 (0.71) and 111 (0.71) employing benign and toxic visuals, respectively. Interestingly, the lowest and highest scores are 0.65 and 0.73, implying that if generalized-toxic in-context examples are incorporated, the performance across all categories tends to converge.

LLaVA-M: In the *self-reflective* scenario for LLaVA-M, toxic visuals with in-context examples yield notable 2-ASR scores of 0.58 in setup 111, 0.48 in setup 011, 0.47 in setup 010, and 0.45 110. In the *general-toxic* scenario, the highest score is 0.45 for toxic visuals in setup 011, while meme

visuals score 0.43 and 0.41 in configurations 011 and 010, respectively, with general-toxic examples.

MiniGPT4: In the *self-reflective* scenario for MiniGPT4, meme visuals score 0.43 and 0.36 in setups 110 and 010, respectively. Toxic visuals achieve 2-ASR scores of 0.41 in setup 010, 0.35 in setup 111, and 0.34 in setup 011. In contrast, the *general-toxic* scenario's highest scores are 0.54 in setup 110 using toxic visuals, 0.52 in setup 011 utilizing meme based visuals, and 0.50 in setup 110 employing benign visual inputs.

The observations from LLaVA-V are consistent with those from LLaVA-M and MiniGPT4, although the scores may differ in scale.

IX. CONCLUSION

We investigate three key factors influencing inappropriate responses in a VLM: (a) visual information, (b) adversarial examples, and (c) positively framed response starters. Adversarial examples are divided into (i) self-reflective and (ii) generalized-toxic categories. We introduce a novel jailbreak method, SKIP-CON, using a skip-connection between two layers and a two-phase evaluation metric. Testing all factor combinations with and without SKIP-CON reveals that each influencing factor can enhance the success rate in jailbreaks. With SKIP-CON, the generalized-toxic in-context examples play the most important role. Even benign images often lead to inappropriate outputs. Visual descriptions help more than positive start phrases. For meme visuals, performance with generalized-toxic examples and descriptions matches that on toxic visuals. Given text's dominant influence over visuals, future work will explore multiple visual inputs to better assess their impact.

REFERENCES

- [1] X. Wang, X. Zhang, Z. Luo, Q. Sun, Y. Cui, J. Wang, F. Zhang, Y. Wang, Z. Li, Q. Yu *et al.*, "Emu3: Next-token prediction is all you need," *arXiv preprint arXiv:2409.18869*, 2024.
- [2] C. Team, "Chameleon: Mixed-modal early-fusion foundation models," *arXiv preprint arXiv:2405.09818*, 2024.
- [3] J. Zhang, J. Huang, S. Jin, and S. Lu, "Vision-language models for vision tasks: A survey," *IEEE Transactions on Pattern Analysis and Machine Intelligence*, vol. 46, no. 8, pp. 5625–5644, 2024.
- [4] J. Achiam, S. Adler, S. Agarwal, L. Ahmad, I. Akkaya, F. L. Aleman, D. Almeida, J. Altenschmidt, S. Altman, S. Anadkat *et al.*, "Gpt-4 technical report," *arXiv preprint arXiv:2303.08774*, 2023.
- [5] Z.-X. Jin, H. Wu, C. Yang, F. Zhou, J. Qin, L. Xiao, and X.-C. Yin, "Ruart: A novel text-centered solution for text-based visual question answering," *IEEE Transactions on Multimedia*, vol. 25, pp. 1–12, 2023.
- [6] D. Xue, S. Qian, Q. Fang, and C. Xu, "Linin: Logic integrated neural inference network for explanatory visual question answering," *IEEE Transactions on Multimedia*, vol. 27, pp. 16–27, 2025.
- [7] X. Lan, J. Xue, J. Qi, D. Jiang, K. Lu, and T.-S. Chua, "Exp1lm: Towards chain of thought for facial expression recognition," *IEEE Transactions on Multimedia*, pp. 1–14, 2025.
- [8] A. Zou, Z. Wang, N. Carlini, M. Nasr, J. Z. Kolter, and M. Fredrikson, "Universal and transferable adversarial attacks on aligned language models," *arXiv preprint arXiv:2307.15043*, 2023.
- [9] X. Gao, X. Wang, Z. Chen, W. Zhou, and S. C. H. Hoi, "Knowledge enhanced vision and language model for multi-modal fake news detection," *IEEE Transactions on Multimedia*, vol. 26, pp. 8312–8322, 2024.
- [10] H. Liu, C. Li, Y. Li, B. Li, Y. Zhang, S. Shen, and Y. J. Lee, "Llavanext: Improved reasoning, ocr, and world knowledge," 2024.
- [11] J. Bai, S. Bai, S. Yang, S. Wang, S. Tan, P. Wang, J. Lin, C. Zhou, and J. Zhou, "Qwen-vl: A versatile vision-language model for understanding, localization," *Text Reading, and Beyond*, vol. 2, 2023.

- [12] S. Hu, Y. Tu, X. Han, C. He, G. Cui, X. Long, Z. Zheng, Y. Fang, Y. Huang, W. Zhao *et al.*, “Minicpm: Unveiling the potential of small language models with scalable training strategies,” *arXiv preprint arXiv:2404.06395*, 2024.
- [13] Z. Khan, B. Vijay Kumar, X. Yu, S. Schuler, M. Chandraker, and Y. Fu, “Single-stream multi-level alignment for vision-language pretraining,” in *European Conference on Computer Vision*. Springer, 2022, pp. 735–751.
- [14] J. Lu, D. Batra, D. Parikh, and S. Lee, “Vilbert: Pretraining task-agnostic visiolinguistic representations for vision-and-language tasks,” *Advances in neural information processing systems*, vol. 32, 2019.
- [15] A. Agrawal, D. Teney, and A. Nematzadeh, “Vision-language pretraining: Current trends and the future,” in *Proceedings of the 60th Annual Meeting of the Association for Computational Linguistics: Tutorial Abstracts*, 2022, pp. 38–43.
- [16] Y. Du, Z. Liu, J. Li, and W. X. Zhao, “A survey of vision-language pre-trained models,” *arXiv preprint arXiv:2202.10936*, 2022.
- [17] S. Khan, M. Naseer, M. Hayat, S. W. Zamir, F. S. Khan, and M. Shah, “Transformers in vision: A survey,” *ACM computing surveys (CSUR)*, vol. 54, no. 10s, pp. 1–41, 2022.
- [18] Y. Weng, W. He, J. Dong, Chaomurilige, X. Liu, and Z. Liu, “Cross-lingual adaptation for vision-language model via multimodal semantic distillation,” *IEEE Transactions on Multimedia*, pp. 1–14, 2025.
- [19] Z. Yin, M. Ye, T. Zhang, T. Du, J. Zhu, H. Liu, J. Chen, T. Wang, and F. Ma, “Vlattack: Multimodal adversarial attacks on vision-language tasks via pre-trained models,” *Advances in Neural Information Processing Systems*, vol. 36, pp. 52936–52956, 2023.
- [20] J. Chen, Y. Jiang, D. Yang, M. Li, J. Wei, Z. Qian, and L. Zhang, “Can llms’ tuning methods work in medical multimodal domain?” in *International Conference on Medical Image Computing and Computer-Assisted Intervention*. Springer, 2024, pp. 112–122.
- [21] N. Carlini, M. Nasr, C. A. Choquette-Choo, M. Jagielski, I. Gao, P. W. Koh, D. Ippolito, F. Tramèr, and L. Schmidt, “Are aligned neural networks adversarially aligned?” *Advances in Neural Information Processing Systems*, vol. 36, pp. 61478–61500, 2023.
- [22] Y. Zhang, T. T. Tzun, L. W. Hern, H. Wang, and K. Kawaguchi, “On copyright risks of text-to-image diffusion models,” *arXiv preprint arXiv:2311.12803*, 2023.
- [23] X. He, L. Lyu, Q. Xu, and L. Sun, “Model extraction and adversarial transferability, your bert is vulnerable!” *arXiv preprint arXiv:2103.10013*, 2021.
- [24] H. Liu, C. Cai, and Y. Qi, “Expanding scope: Adapting english adversarial attacks to chinese,” *arXiv preprint arXiv:2306.04874*, 2023.
- [25] J. Lin, J. Zou, and N. Ding, “Using adversarial attacks to reveal the statistical bias in machine reading comprehension models,” *arXiv preprint arXiv:2105.11136*, 2021.
- [26] W. E. Zhang, Q. Z. Sheng, A. Alhazmi, and C. Li, “Adversarial attacks on deep-learning models in natural language processing: A survey,” *ACM Transactions on Intelligent Systems and Technology (TIST)*, vol. 11, no. 3, pp. 1–41, 2020.
- [27] C. Anil, E. Durmus, N. Panickssery, M. Sharma, J. Benton, S. Kundu, J. Batson, M. Tong, J. Mu, D. Ford *et al.*, “Many-shot jailbreaking,” *Advances in Neural Information Processing Systems*, vol. 37, pp. 129696–129742, 2024.
- [28] T. Q. Tran, K. Wataoka, and T. Takahashi, “Initial response selection for prompt jailbreaking using model steering,” in *ICLR 2024 Workshop on Secure and Trustworthy Large Language Models*, 2024.
- [29] J. Ji, M. Liu, J. Dai, X. Pan, C. Zhang, C. Bian, B. Chen, R. Sun, Y. Wang, and Y. Yang, “Beavertails: Towards improved safety alignment of llm via a human-preference dataset,” *Advances in Neural Information Processing Systems*, vol. 36, pp. 24678–24704, 2023.
- [30] M. S. Hee, S. Sharma, R. Cao, P. Nandi, P. Nakov, T. Chakraborty, and R. K.-W. Lee, “Recent advances in online hate speech moderation: Multimodality and the role of large models,” in *Findings of the Association for Computational Linguistics: EMNLP 2024*, Y. Al-Onaizan, M. Bansal, and Y.-N. Chen, Eds. Miami, Florida, USA: Association for Computational Linguistics, Nov. 2024, pp. 4407–4419. [Online]. Available: <https://aclanthology.org/2024.findings-emnlp.254/>
- [31] P. Nandi, S. Sharma, and T. Chakraborty, “Safe-meme: Structured reasoning framework for robust hate speech detection in memes,” *arXiv preprint arXiv:2412.20541*, 2024.
- [32] H. Liu, C. Li, Q. Wu, and Y. J. Lee, “Visual instruction tuning,” *Advances in neural information processing systems*, vol. 36, pp. 34892–34916, 2023.
- [33] H. Liu, C. Li, Y. Li, and Y. J. Lee, “Improved baselines with visual instruction tuning,” in *Proceedings of the IEEE/CVF Conference on Computer Vision and Pattern Recognition*, 2024, pp. 26296–26306.
- [34] D. Zhu, J. Chen, X. Shen, X. Li, and M. Elhoseiny, “Minigpt-4: Enhancing vision-language understanding with advanced large language models,” *arXiv preprint arXiv:2304.10592*, 2023.
- [35] S. Zhu, R. Zhang, B. An, G. Wu, J. Barrow, Z. Wang, F. Huang, A. Nenkova, and T. Sun, “Autodan: interpretable gradient-based adversarial attacks on large language models,” *arXiv preprint arXiv:2310.15140*, 2023.
- [36] E. Jones, A. Dragan, A. Raghunathan, and J. Steinhardt, “Automatically auditing large language models via discrete optimization,” in *International Conference on Machine Learning*. PMLR, 2023, pp. 15307–15329.
- [37] Y. Liu, S. Mao, X. Mei, T. Yang, and X. Zhao, “Sensitivity of adversarial perturbation in fast gradient sign method,” in *2019 IEEE Symposium Series on Computational Intelligence (SSCI)*, 2019, pp. 433–436.
- [38] E. Shayegani, Y. Dong, and N. Abu-Ghazaleh, “Jailbreak in pieces: Compositional adversarial attacks on multi-modal language models,” *arXiv preprint arXiv:2307.14539*, 2023.
- [39] Z. Zhang, G. Shen, G. Tao, S. Cheng, and X. Zhang, “Make them spill the beans! coercive knowledge extraction from (production) llms,” *arXiv preprint arXiv:2312.04782*, 2023.
- [40] Y. Du, S. Zhao, M. Ma, Y. Chen, and B. Qin, “Analyzing the inherent response tendency of llms: Real-world instructions-driven jailbreak,” *arXiv preprint arXiv:2312.04127*, 2023.
- [41] X. Yang, X. Wang, Q. Zhang, L. Petzold, W. Y. Wang, X. Zhao, and D. Lin, “Shadow alignment: The ease of subverting safely-aligned language models,” *arXiv preprint arXiv:2310.02949*, 2023.
- [42] X. Qi, Y. Zeng, T. Xie, P.-Y. Chen, R. Jia, P. Mittal, and P. Henderson, “Fine-tuning aligned language models compromises safety, even when users do not intend to!” *arXiv preprint arXiv:2310.03693*, 2023.
- [43] S. Lermen, C. Rogers-Smith, and J. Ladish, “Lora fine-tuning efficiently undoes safety training in llama 2-chat 70b,” *arXiv preprint arXiv:2310.20624*, 2023.
- [44] X. Li, Z. Zhou, J. Zhu, J. Yao, T. Liu, and B. Han, “Deepinception: Hypnotize large language model to be jailbreaker,” *arXiv preprint arXiv:2311.03191*, 2023.
- [45] P. Ding, J. Kuang, D. Ma, X. Cao, Y. Xian, J. Chen, and S. Huang, “A wolf in sheep’s clothing: Generalized nested jailbreak prompts can fool large language models easily,” *arXiv preprint arXiv:2311.08268*, 2023.
- [46] Z. Wei, Y. Wang, A. Li, Y. Mo, and Y. Wang, “Jailbreak and guard aligned language models with only few in-context demonstrations,” *arXiv preprint arXiv:2310.06387*, 2023.
- [47] J. Wang, Z. Liu, K. H. Park, Z. Jiang, Z. Zheng, Z. Wu, M. Chen, and C. Xiao, “Adversarial demonstration attacks on large language models,” *arXiv preprint arXiv:2305.14950*, 2023.
- [48] D. Kiela, H. Firooz, A. Mohan, V. Goswami, A. Singh, P. Ringshia, and D. Testuggine, “The hateful memes challenge: Detecting hate speech in multimodal memes,” *Advances in neural information processing systems*, vol. 33, pp. 2611–2624, 2020.
- [49] A. Deng, T. Cao, Z. Chen, and B. Hooi, “Words or vision: Do vision-language models have blind faith in text?” *arXiv preprint arXiv:2503.02199*, 2025.
- [50] A. Vaswani, N. Shazeer, N. Parmar, J. Uszkoreit, L. Jones, A. N. Gomez, Ł. Kaiser, and I. Polosukhin, “Attention is all you need,” *Advances in neural information processing systems*, vol. 30, 2017.
- [51] J. L. Ba, J. R. Kiros, and G. E. Hinton, “Layer normalization,” *arXiv preprint arXiv:1607.06450*, 2016.
- [52] J. Zhuo, S. Zhang, X. Fang, H. Duan, D. Lin, and K. Chen, “Prosa: Assessing and understanding the prompt sensitivity of llms,” *arXiv preprint arXiv:2410.12405*, 2024.
- [53] S. Anagnostidis and J. Bulian, “How susceptible are llms to influence in prompts?” *arXiv preprint arXiv:2408.11865*, 2024.
- [54] A. Wei, N. Haghtalab, and J. Steinhardt, “Jailbroken: How does llm safety training fail?” *Advances in Neural Information Processing Systems*, vol. 36, pp. 80079–80110, 2023.
- [55] A. Ardit, O. Obeso, A. Syed, D. Paleka, N. Panickssery, W. Gurnee, and N. Nanda, “Refusal in language models is mediated by a single direction,” *arXiv preprint arXiv:2406.11717*, 2024.
- [56] A. . M. Llama Team, “The llama 3 family of models,” https://github.com/meta-llama/PurpleLlama/blob/main/Llama-Guard3/1B/MODEL_CARD.md, 2024.

SUPPLEMENTARY INFORMATION

A. Preliminary Observations on Distinguishability of Benign and Toxic inputs in Meta-Llama-3-8B-Instruct

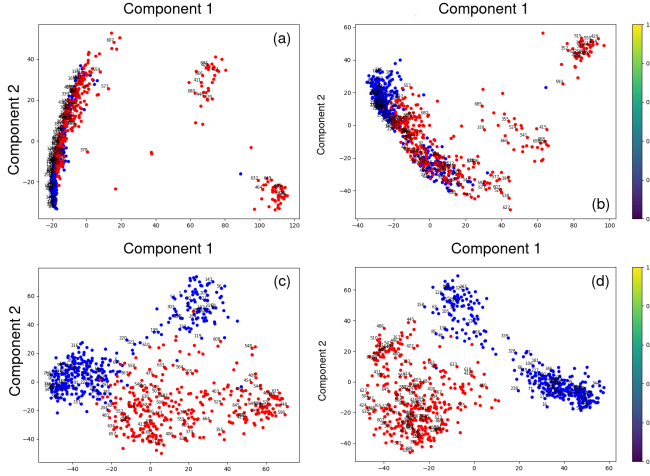


Fig. 1: An illustration of layer-wise representation of toxic (red) and benign (blue) input prompts for model Meta-Llama-3-8B-Instruct: (a) In the initial layer, toxic and benign inputs are indistinguishable. (b) The indistinguishability persists up to the third layer. (c) At the fourth layer, distinct clusters appear and (d) The separation remains evident up to the final layer.

In a decoder-only model M_θ , given an input X , the output Y is a sequence of tokens that is generated in an auto-regressive manner. The term ‘autoregression’ indicates that each token is predicted based on the input and previously generated tokens. Mathematically, it can be expressed as,

$$P(Y|X) = \prod_{t=1}^T P(y_t|y_{<t}, X; \theta) \quad (7)$$

where, θ represents the parameters of the model M_θ , the previously generated tokens are denoted by $y_{<t}$, and $P(y_t | y_{<t}, X; \theta)$ is computed using the decoder’s softmax layer over its vocabulary. The hidden state at each time step t is obtained through the decoder layers.

$$h_t = f(y_{<t}, X; \theta) \quad (8)$$

where $f(\cdot)$ represents the transformation performed by the self-attention and feedforward layers. Here, we plot the hidden state of the *final* token into two-dimensional space. Figure 1 presents the layer-wise representation of toxic and benign input prompts in Meta-Llama-3-8B-Instruct. To isolate the internal representations of *input prompts* from the corresponding *responses*, the maximum number of new token generation is limited to one. Figure 1.a illustrates that the initial layer fails to discriminate between the internal representations of benign and toxic inputs. The indistinguishability persists up to the *third* layer (c.f. Figure 1.b) but at the *fourth* layer, as shown in Figure 1.c, the internal representations appear more discriminative and tend to form clusters. The distinction persists till the last layer (c.f. Figure 1.d).

B. Observation for text-based Inputs

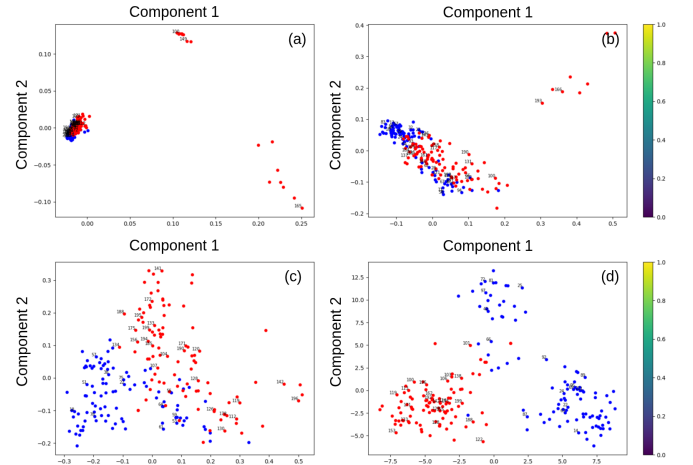


Fig. 2: An illustration of internal representations for toxic (red) and benign (blue) prompts in LLaVA-M: (a) the first layer doesn’t exhibit any separation, (b) by the 3rd layer distinct clusters corresponding to the benign and toxic prompts begin to emerge; (c) surprisingly a clear distinction appears at the fourth layer, which (d) gradually matures and persists to the final layer.

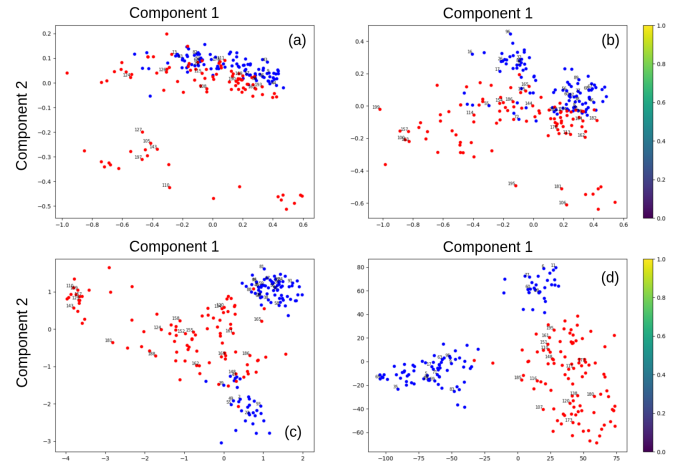


Fig. 3: An illustration of internal representations for toxic (red) and benign (blue) prompts in MiniGPT4: (a) the initial layer fails to differentiate benign prompts from the toxic ones, (b) by the 3rd layer respective clusters for both the benign and toxic prompts starts to emerge; (c) a clear distinction appears at the seventh layer, that (d) gradually matures and remains intact till the last layer.

C. Observation for Image-based Inputs

The benign and each subcategory of toxic class, contains a total of 100 visual instances. Each row in Figure 4, Figure 5, and Figure 6 presents a comparative analysis between a specific toxicity subcategory and benign examples for LLaVA-V, LLaVA-M, and MiniGPT4, respectively; it describes the

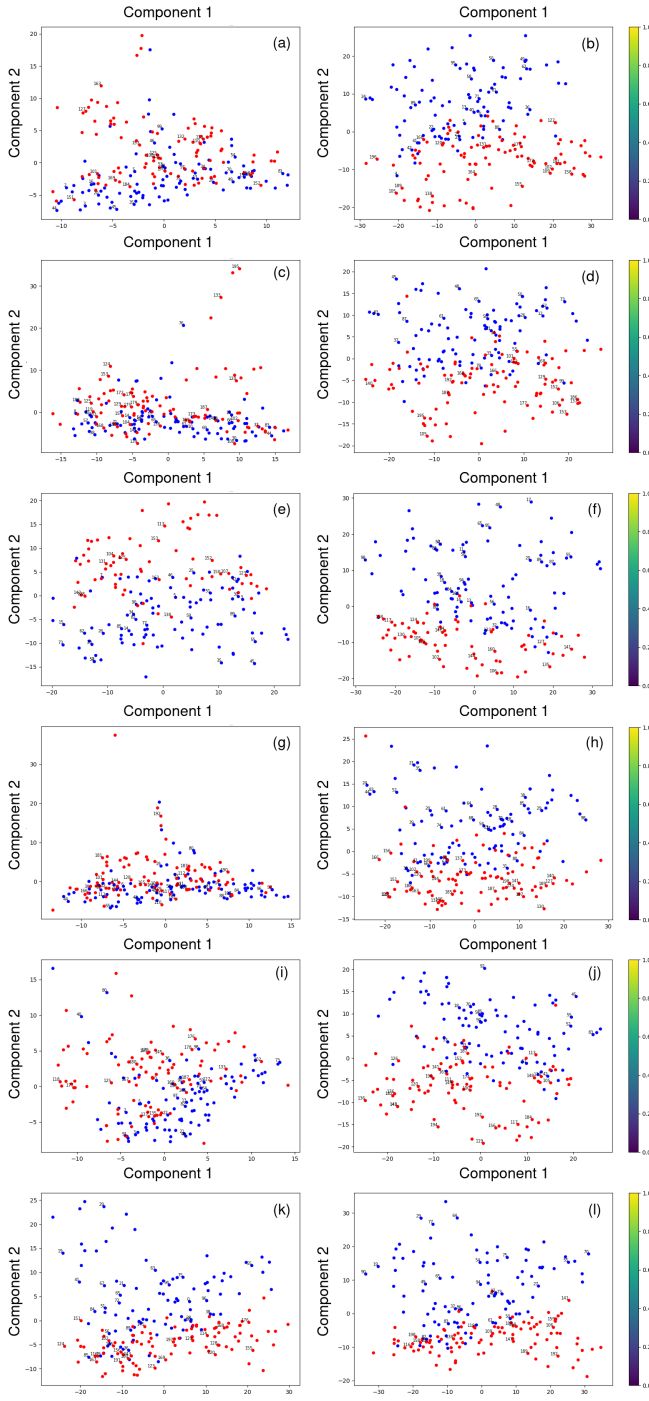


Fig. 4: An illustration of the internal representations of toxic (red) and benign (blue) visual inputs for the model LLaVA-V, across various targeted communities. Subfigures (a)–(b) distinguish between toxic memes targeting *women* and benign images; (c)–(d) present similar contrasts for the *African-American* community; (e)–(f) focus on memes directed at *disabled* individuals; (g)–(h) examine toxic content related to *Islam*; and (i)–(j) address toxic representations targeting the *LGBTQ* community. Lastly, (k)–(l) compare *general toxic* visual inputs with benign counterparts.

specific layers in the model where the differentiation between toxic and benign images emerges, highlighting the stages where these distinctions become visually prominent.

Figure 4 provides an analysis of benign images and toxic memes across different categories. Subfigures (a) and (b) illustrate the differentiation between toxic memes targeting the benign and the women category, with separation emerging in the 14th layer and reaching optimality at the 23rd layer. A similar trend is observed in the subfigures (c) and (d), where the distinction for the African-American black community appears later, beginning at the 19th layer and optimizing at the 22nd layer. In subfigures (e) and (f), the analysis is based on the disabled individuals, with initial differentiation observed in the 21st layer and maturing at the 24th layer. For toxic visual content related to Islam (c.f. Figure 4(g) and h), the distinction emerges at the 17th layer and peaks at the 22nd layer. Subfigures (i) and (j) depict the contrast between toxic memes directed at the LGBTQ community and benign images, where an early separation is observed at the 10th layer, optimizing at the 22nd layer. Lastly, figure 4.k and 4.l examine the general toxic visual instances versus benign images, with the distinction appearing relatively late at the 22nd layer and reaching its optimal separation at the 23rd layer. For both general toxic and meme visuals, the separation becomes prominent between 21st to 24th layer.

Figure 5 illustrates the separability between various sub-groups of toxic memes and benign visual inputs in LLaVA-M. Subfigures (a)–(b), (c)–(d), (e)–(f), (g)–(h), (i)–(j), and (k)–(l) correspond to memes targeting women, African-Americans, individuals with disabilities, the Islamic community, the LGBTQ community, and general toxic content, respectively. In all the mentioned sub-categories—excluding LGBTQ community and general toxic visuals, the separation between toxic and benign inputs is clear from the initial layer and remains consistently distinguishable through to the final layer. In case of LGBTQ community and the general toxic visuals, the benign and toxic input visuals are identifiable after third and 14th layer, respectively.

Interestingly, a similar pattern to that observed in LLaVA-M emerges in MiniGPT4, particularly in the visual representations across meme sub-categories when compared to benign counterparts (c.f. Figure 6). Subfigures (a)–(b), (c)–(d), (e)–(f), (g)–(h), (i)–(j), and (k)–(l) correspond to memes targeting women, African-Americans, individuals with disabilities, the Islamic community, the LGBTQ community, and general toxic content, respectively. For MiniGPT4, across all examined sub-categories, the distinction between toxic and benign inputs is apparent from the initial layer and remains consistent throughout all the remaining layers up to the final one.

D. Preliminary Observation on Attention Scores for Image-based Inputs in LLaVA-V

Additionally, we examined the attention scores when an unsafe input is prompted with benign, toxic, and meme-based visual content. Figure 7 and 8 demonstrates the average cross-attention scores across all layers for model, LLaVA-V and LLaVA-M when unsafe textual prompts paired with different

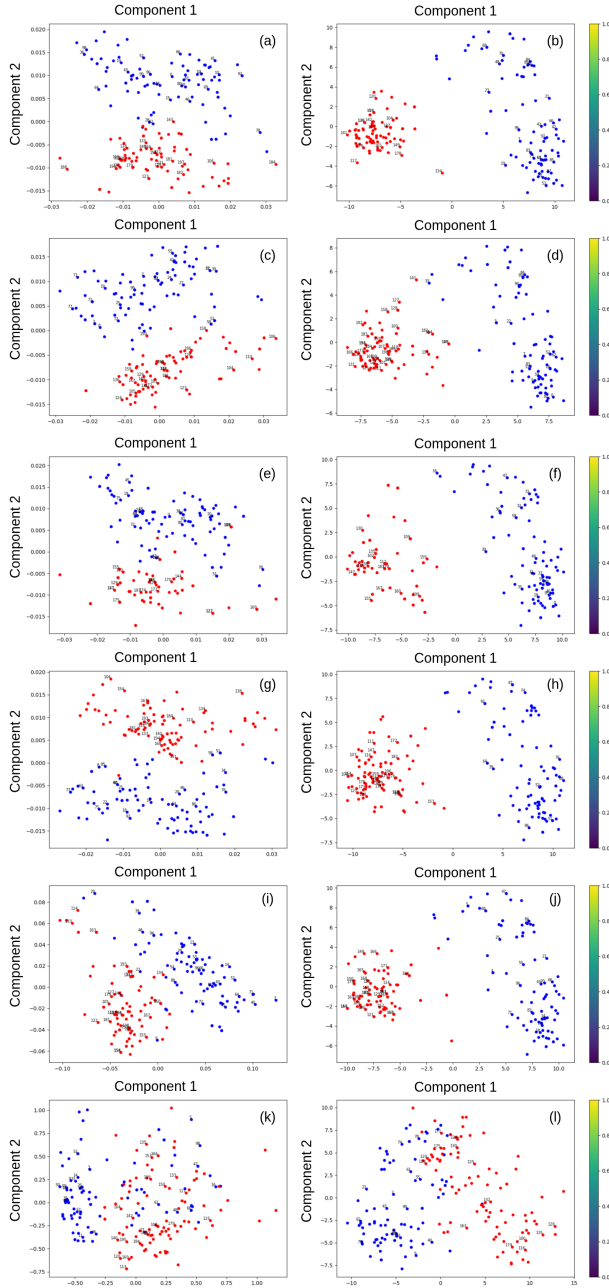


Fig. 5: An illustration of internal representations of toxic (red) and benign (blue) visual inputs (only) for model LLaVA-M across different targeted communities: (a)–(b) show the distinction between toxic memes targeting the women and benign images, (c)–(d) illustrate a similar trend for toxic memes targeting the African-American community, (e)–(f) analyze toxic memes directed at disabled individuals, (g)–(h) examine toxic visual content related to Islam, (i)–(j) depict toxic memes targeting the LGBTQ community. Finally, (k)–(l) compare general toxic visual instances against benign images.

categories of visual inputs. In the case of LLaVA-V, for toxic visuals, the average attention scores demonstrate a gradual increment over benign visuals (c.f. Figure 7.(a)) that is consistent with the observations in Figure 4. Interestingly, the average

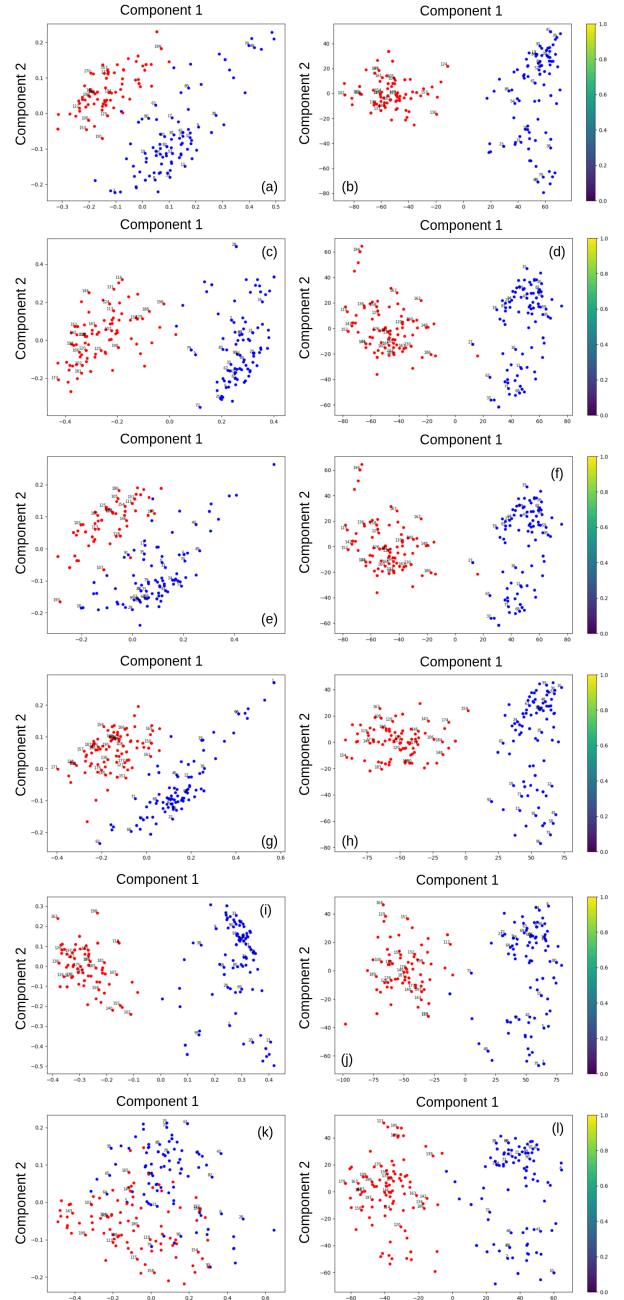


Fig. 6: An illustration of internal representations of toxic (red) and benign (blue) visual inputs (only) for model MiniGPT4 across different targeted communities: (a)–(b) show the distinction between toxic memes targeting the women and benign images, (c)–(d) illustrate a similar trend for toxic memes targeting the African-American community, (e)–(f) analyze toxic memes directed at disabled individuals, (g)–(h) examine toxic visual content related to Islam, (i)–(j) depict toxic memes targeting the LGBTQ community. Finally, (k)–(l) compare general toxic visual instances against benign images.

attention scores for meme-based visuals are higher (or equal) than benign visuals, starting from the initial layer (c.f. Figure 7.(b)). Interestingly, the average cross-attention scores for the toxic and meme visuals are consistently lower than benign

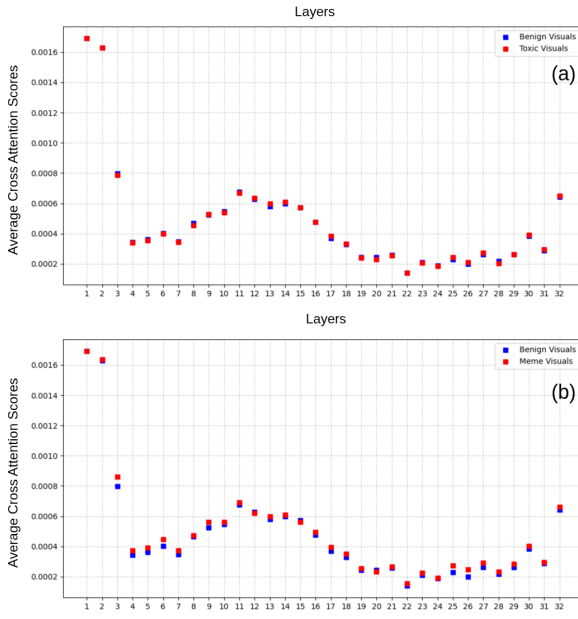


Fig. 7: An illustration of the influence of visual inputs on attention scores when prompted with unsafe queries for LLaVA-V: (a) shows the average cross-attention scores elicited by unsafe textual prompts when paired with either benign or toxic images, (b) demonstrates the same when paired with either benign or meme images.

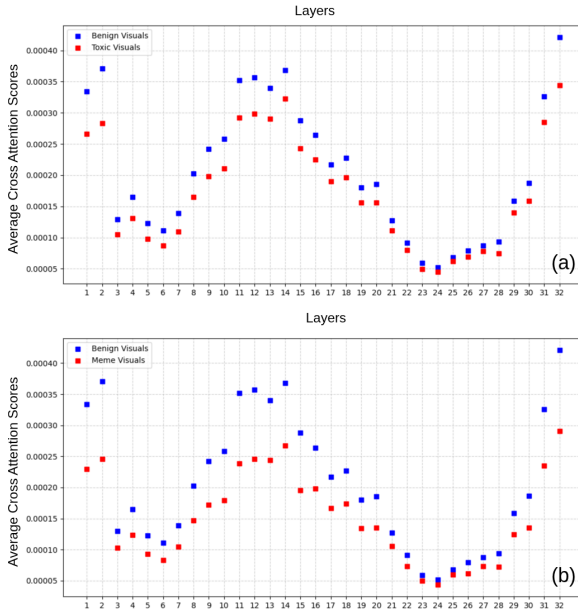


Fig. 8: An illustration of the influence of visual inputs on attention scores when prompted with unsafe queries for LLaVA-M: (a) shows the average cross-attention scores elicited by unsafe textual prompts when paired with either benign or toxic images, (b) demonstrates the same when paired with either benign or meme images.

effective as toxic visuals in a successful jailbreak.

visuals in LLaVA-M (c.f. Figure 8). This observation endorses the hypothesis that memes-based visuals can be equivalently